УДК 539.4

K. Gergely, S. Gabor, R. Tamas

CFD.HU Ltd., Budapest, Hungary

SIMULATION OF TWO-PHASE FLOW ON SHELL SIDE OF VVER-440 SECONDARY BOILERS

Shell side flow in VVER-440 steam generators has been simulated by using two-dimensional and three-dimensional geometrical approach. A number of operating states have been analyzed: nominal and increased power load with the original feed water injection (within the tube bank) and with presently used water injection (above the tube bank). The mathematical model involves physical effects such as: thermal expansion of water phase, local condensation in the region of feed water injection (mixed pre/heater tank), variable slip velocity of the bubbly phase depending on local volume fraction of steam, spatial variation of the water level above the tube bank settling of disperse corrosion product under the tube bank. Micro-models have been developed for calculation of anisotropic resistance of the tube bank and pipe supports, local heat flux over the tube surfaces and the spatial variation of water injection intensity. Water surface elevation and disperse phase deposition patterns are in line with measured data published in scientific literature [3], [4].

Keywords: simulation, two-phase flow, VVER-440, steam generator.

1. Introduction. Inefficient blow down is one of the known design problems of VVER-440 type secondary boilers. Since secondary boilers are critical parts from the point of view of the prolongation of life cycle, the improvement of mud extraction efficiency has been issued by NPP Paks. The blow down system is aimed at the extraction of ionic and disperse contaminants from the steam generator vessel. In order to achieve high blow down efficiency, the extraction outlet need to be placed at the point of highest contaminant concentration [5]. LG Energy Ltd. has been contracted by NPP Paks for the improvement of blow down efficiency, analyses of shell side flow and transport processes has been carried out by CFD.HU Ltd. as a subcontractor.

The most important effect concerning the shell side flow in a secondary boiler is the unevenness of heating. Every steam generator contains 5536 pipes of 16 mm external diameter bended in horizontal planes. With the help of the enthalpy of the primary circuit coolant delivered by the pipes secondary circuit water is heated up to saturation temperature and evaporated on the shell side of the pipes. In the vicinity of the hot leg (inlet collector) temperature of the primary circuit water and the consequential heat flux is higher then those at the cold leg (outlet collector). Unevenness of steam production due to the spatial variation of heat flux is the driver of the shell side circulation. Pipe supports placed in planes perpendicular to the axis of the vessel has a significant resistance against the axial flow component thus the circulation is forced into cross-sectional planes (nearly 2D flow). Really three-dimensional flow takes place only at the end walls of the vessel, in the vicinity of the collector. Circulation intensity is limited by the shell side resistance of the tube bank and by the admittance of the relatively large gap

between the tube bank and the vessel wall. Spatial distribution of the heat flux has been obtained from pipe wise coupled 1D thermo-hydraulic model. Anisotropic shell side resistance of the tube bank and the resistance of pipe supports have been calculated by using 2D and 3D micro-models.

Due to the overheating of water phase the bubbles are growing while rising towards the surface. In regions characterized by high local void fraction the bubble agglomeration process can occur as well further increasing the bubble size. Owing to these effects the difference between bubbly phase and liquid phase velocities (slip velocity) varies. In order to obtain accurate representation of surface shape and vapor distribution, the local value of slip velocity has been obtained from a mathematical model based on measured correlations.

Feed water injection has a large impact on shall side circulation as well. 9.3% of the heat power is spent on pre-heating of feed water to saturation temperature. This is mostly covered by latent heat released by the bubbly vapor phase during local condensation processes. Since the energy demand of feed water decreases the vapor content and the specific volume, feed water drops downwards from the injection point. For the accurate representation of pre-heating and steam generation processes a special multi-phase flow model fulfilling local mass and energy balances has been developed and implemented in ANSYS-FLUENT simulation system in the form of User Defined Functions (UDF-s).

Numerical simulation of the multiphase flow provides complete image about the spatial distributions of velocity and void fraction, thus allowing detailed analysis of the sedimentation of disperse corrosion products and providing data essential for improvement of blow down efficiency. Numerous further application of the Computational Fluid Dynamic (CFD) model is foreseeable.

2. Geometrical model, mesh and boundary conditions. Three-dimensional meshes of two different resolution and a two-dimensional (cross-section) mesh have been developed. The latter has been found very useful in the work phase of simulation model development. Time dependent (unsteady) simulation has been carried out in every case with sufficient number of time steps for achieving converged solution.

Our most detailed 3D model is illustrated in Fig. 1. The number of computational cells is 1.2 million. The geometrical model contains both the new and the old feed water supply collectors. The simplified 3D model consist of 0,5 million cells. In order to reduce the number of cells the feed water collectors, some inclined rows of pipe supports at the vessel ends, together with some details of minor importance have been omitted from the model. By using the converged results of the simplified model as initial condition for the finely resolved model 5 fold reduction of the computation time could be achieved.

Number of cells in the 2D model was 4100, therefore the computing time is about 100 times shorter relative to the simplified 3D model, which has been found very helpful when developing the mathematical description of slip velocity and phase changes, moreover, the 2D simulation gave meaningful results in the investigated cross-section due to the nearly two-dimensional nature of then flow.

The uppermost part of vessel together with the droplet separator has been omitted from the model. The upper boundary condition has been placed well above the water surface, therefore the liquid water content of the flow was nearly zero at the outlet. Water surface elevation has been locally obtained from dynamics of

phase separation. Rigid, adiabatic wall boundary conditions have been used for modeling the remaining part of the vessel wall. Further mass, momentum and energy exchange processes have been described with spatially distributed volume sources. Specification of the source terms will discussed in the next chapter.

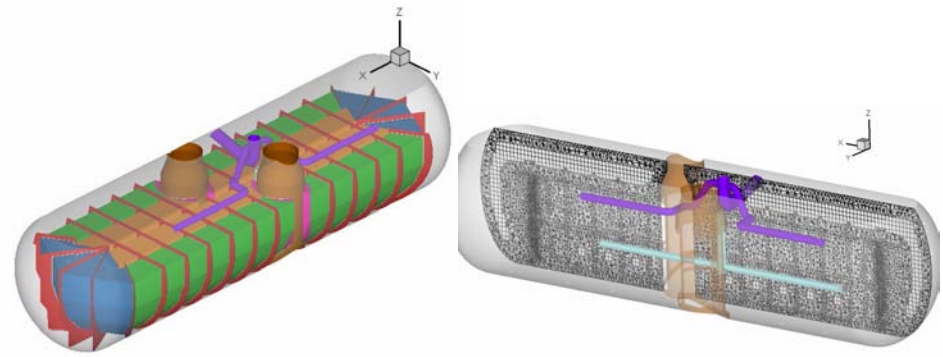

Fig. 1. The geometrical model (left) and the numerical mesh (right).

3. Mathematical model.

3.1. Heating. Shell side water circulation in the steam generator vessel is driven by heat flux received from the heat exchanger tubes and the consequential increase in the specific volume of the fluid, which is 6.7% in the case of feed water pre-heating and a factor of 33.8 in the case of evaporation.

Heating intensity can be computed on the basis of coupled modeling of primary and secondary circuit processes. Pressure drop between the hot and cold collector uniformly effects every heat exchanger pipes, therefore the tubes can be regarded as different hydraulic resistances in parallel connection. Diameter and wall thickness is identical for every pipe but pipe lengths vary between 8.3 m (inner pipes) and 12.5 m (outer pipes). The shorter pipes deliver more water with smaller temperature drop along the pipe. In view of the mass flow-rate values, the cooling curves and heat flux distribution could be calculated for each individual pipes. Constant value of the shell side surface heat transfer coefficient has been assumed. Outlet temperature of the primary circuit water has been calculated as the mass weighted average of the pipe outlet temperatures.

Potentially the exact locations of inactive (plugged) pipes can be taken into account in the model. Presently a power density distribution for randomly distributed plugged pipes (58 pipes out of 5478) has been taken into account (see Fig. 2.).

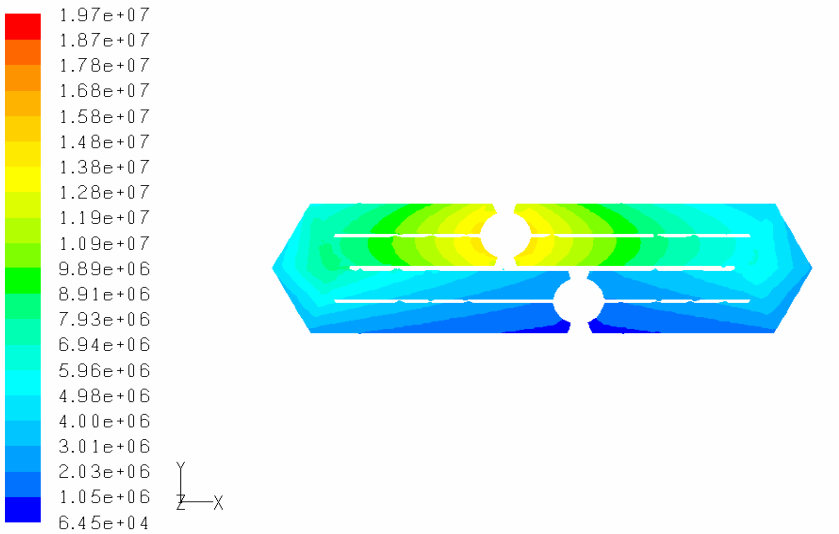

Fig. 2. Power density distribution in Wm^{-3}.

3.2. Hydraulic resistance of the tube bank and pipe supports. ANSYS-FLUENT simulation system provides anisotropic model for porous media flows. Pressure gradient is calculated by means of Eq. 1.:

$$\vec{F} = -\left(\mu \cdot \vec{\vec{D}} \cdot \vec{v}' + \frac{1}{2} \cdot \rho \cdot \left| \vec{v}' \right| \cdot \vec{\vec{C}} \cdot \vec{v}' \right), \tag{1}$$

velocity $\vec{v}' = \gamma \cdot \vec{v}$ in Eq. 1 is the physical velocity in porous medium of γ blocking ratio, $\vec{\vec{D}}$ and $\vec{\vec{C}}$ are symmetric tensors of resistance coefficients specified on the basis of characteristic directions (symmetries) of the medium.

Tube banks of the steam generators has been modeled as a porous zone of variable resistance matrices obtained from zone by zone 2D micro modeling of the flow. Pipe supports have been taken into account as porous surfaces (pressure jumps). Resistance coefficient has been identified via 3D micro modeling by assuming periodicity both horizontal and vertical direction.

3.3 Pre-heating and evaporation. Feed water injection has been modeled by volume sources active in the vicinity of injection nozzles. Intensity of the volume source has been approximated by a linear function of axial coordinate parameterized on the basis of hydraulic assumptions concerning the feed water collectors. Both the original and the new (see Fig. 3) feed water injection systems can be activated in the simulation model.

The feed water, characterized by a temperature range 223–225°C, mixes with the boiling water (characterized by the saturation temperature 258.7°C and by variable fraction of vapor bubbles) when injected into the vessel.

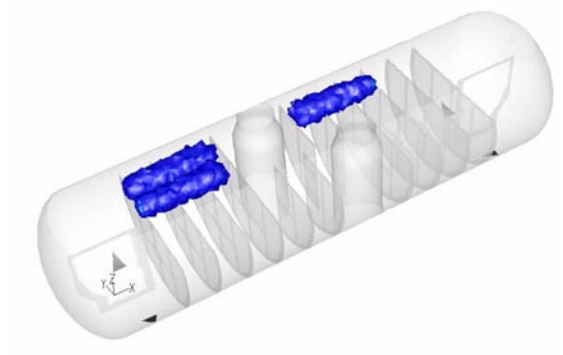

Fig. 3. Feed water injection (new design).

When relatively small portion of feed water is mixed with boiling water of high vapor content, the liquid temperature in the resulting mixture reaches the saturation temperature. When volume fraction of the initial feed water is larger, the vapor content can condense perfectly and the temperature of the resulting mixture can be lower than the saturation temperature. The mixing process can take place within the tube bank too. In this latter case, the additional heat received from the heat exchanger pipes must be taken into account.

This coupled process of pre-heating, condensation and heat exchange with the solid surface has been described by the introduction of a fictive third phase – the feed water phase –to the mathematical model. In every computational cell a mixture of the following phases are present:

Phase 1: saturated vapor – primary phase,
Phase 2: saturated water – secondary phase,
Phase 3: feed water – secondary phase.

Portion of the k-th phase is described by its volume fraction α_k, which is the volume occupied by the k-th phase over the cell volume. Obviously the following implicit condition has to be fulfilled:

$$\sum_{k=1}^{3} \alpha_k = 1. \tag{2}$$

Mixture density and velocity can be calculated from the following formulae:

$$\rho = \sum_{k=1}^{3} \alpha_k \rho_k \ , \tag{3}$$

$$\vec{v} = \frac{1}{\rho} \sum_{k=1}^{3} \alpha_k \rho_k \vec{v}_k \ , \tag{4}$$

in which ρ_k and $\vec{v}_k$ are the density and velocity of the k-th phase.

Simulation has been carried out in ANSYS-FLUENT system, by using multiphase mixture flow model based on the following conservation equations:

Continuity:

$$\frac{\partial \rho}{\partial t} + \nabla \cdot (\rho \vec{v}) = \sum_{k=1}^{3} S_{m,k} \ , \tag{5}$$

in which $S_{m,k}$ is a volume source of mass in kg m^{-3} s^{-1} for the k-th phase. Volume sources can be evaluated in user defined functions written in C programming language. Source terms can be functions of spatial coordinate, time and any field variables used in the mathematical model, which makes the mathematical description of phase change process possible.

In addition to the continuity equation of the mixture the continuity equation must be solved for every secondary phase:

$$\frac{\partial}{\partial t}(\alpha_p \rho_p) + \nabla \cdot (\alpha_p \rho_p \vec{v}_m) = -\nabla \cdot (\alpha_p \rho_p \vec{v}_{dr,p}) + S_{m,p} \ , \tag{6}$$

in which $\vec{v}_{dr,p} = \vec{v}_p - \vec{v}_m$ is the drift velocity for the k-th phase. Volume fraction of primary phase can be evaluated from Eq. 2, therefore the solution of an additional continuity equation is not required.

The momentum equation for the mixture reads:

$$\begin{aligned} \frac{\partial}{\partial t}(\rho \vec{v}) + \nabla \cdot (\rho \vec{v} \cdot \vec{v}) = -\nabla p + \nabla \cdot \left[\mu (\nabla \vec{v} + \nabla \vec{v}^{\,T})\right] + \\ \rho \vec{g} + \vec{F} + \nabla \cdot \left(\sum_{k=1}^{3} \alpha_k \rho_k \vec{v}_{dr,k} \vec{v}_{dr,k} \right). \end{aligned} \tag{7}$$

Number of phases in Eq. 7 is 3. $\vec{F}$ denotes the volume forces (out of the gravitation force), which is the hydraulic resistance of the tube bank in our case. ? is the dynamical viscosity of the mixture including turbulent viscosity. ? is calculated on the following way:

$$\mu = \sum_{k=1}^{m} \alpha_k \mu_k \ . \tag{8}$$

Eq. 5 expression of the continuity equation, Eq. 6 for two secondary phases and the three components of Eq. 7 constitute a system of 6 transport equations for 6 primary scalar unknowns: pressure $p(t, \vec{r})$, volume fraction of two secondary phases $\alpha_p(t, \vec{r})$ and 3 components of the mixture velocity $\vec{v}(t, \vec{r})$.

In thermodynamic equilibrium state, feed water and vapor cannot be present together in the same computational cell. Phase changes have to guide the system

towards the local thermodynamic equilibrium and fulfill the local energy balance. The local thermodynamic equilibrium is quickly restored in the real system due to the intensive mixing, therefore the relaxation time necessary for achieving the thermodynamic equilibrium is estimated by the Δt time step of the simulation. (Processes shorter than one time step can be regarded as sudden changes.) Condensation of the local vapor content leads to the release of the following amount of heat:

$$u_1 = \alpha_1 \rho_1 r_1 / \Delta t \,, \tag{9}$$

in which r_1 is the latent heat of water vapor.

For heating the local feed water content to saturation temperature we need to provide u_3 amount of energy:

$$u_3 = \alpha_3 \rho_3 r_3 / \Delta t \,, \tag{10}$$

$r_3 = -c_{p,3}(T_2 - T_3)$ is the enthalpy difference and $c_{p,3}$ is the specific heat of feed water on constant pressure, T_2 and T_3 are the temperatures of saturated water and feed water.

q denotes the power released by the heat exchanger tubes in unit volume. Conditions on local evaporation and pre-heating can be expressed in the following terms:

A. Evaporation: $q + u_1 + u_3 \geq 0$, (11)

B. Pre-hating: $q + u_1 + u_3 < 0$. (12)

A. In the case of local evaporation the feed water phase need to be completely transformed into saturated water by pre-heating:

$$S_{m,3} = u_3 / r_3 \,, \tag{13}$$

the remaining energy is used for steam production:

$$S_{m,1} = (q + u_3) / r_1 \,. \tag{14}$$

B. When local pre-heating takes place, we remove the local steam phase (by perfect condensation):

$$S_{m,1} = -u_1 / r_1 \,, \tag{15}$$

and the remaining energy can be used for pre-heating:

$$S_{m,3} = (q + u_1) / r_3 \,. \tag{16}$$

Formation rate of saturated water can be calculated from the local mass conservation:

$$S_{m,2} = -S_{m,1} - S_{m,3}. \tag{17}$$

Application of mass sources Eqs. 13–17 in transport equations 5–6 enforces local mass and energy balances during the phase change process. By the application of the 3 phase model together with the above sources the solution of energy equation for temperature can be avoided.

3.4. Slip velocity. Slip velocity of water vapor relative to the liquid phases is calculated from measured correlation [1, 2] depending on local vapor content and the vector sum of gravity and inertial accelerations. Slip velocity in homogenous steady flow for the operating conditions specific to NPP Paks is plotted in Fig. 4 against the local vapor concentration.

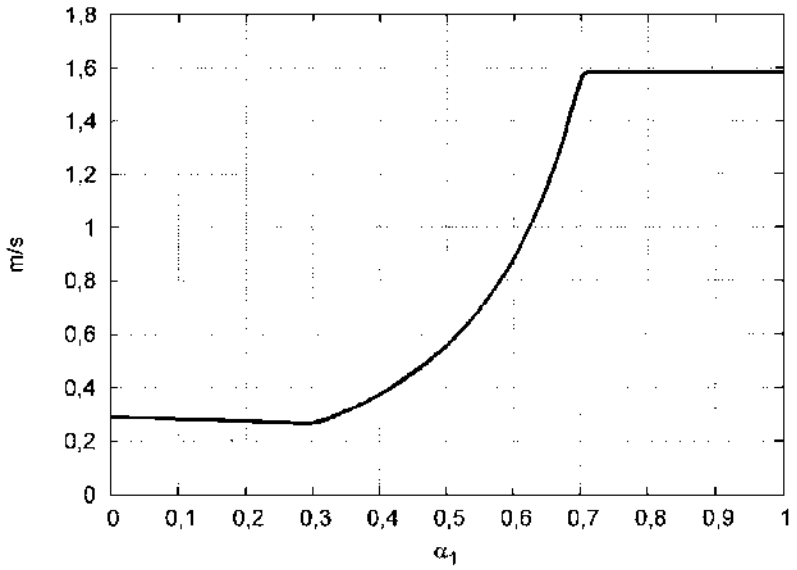

Fig. 4. Slip velocity (difference between velocity of gas and liquid phases) as a function of the volume fraction of gas phase (steam) for homogenous flow with zero inertial forces.

In the flow field of the steam generator large inertial forces occur due to the flow inhomogeneous flow. The resulting slip velocity is plotted in Fig. 5.

The slip velocity formula, employed in this study, provide at least qualitatively correct description of the water droplet sedimentation above the surface. This modeling feature is necessary for realistic formation of water surface which is actually the upper boundary condition for the shell side water circulation in the steam generator vessel.

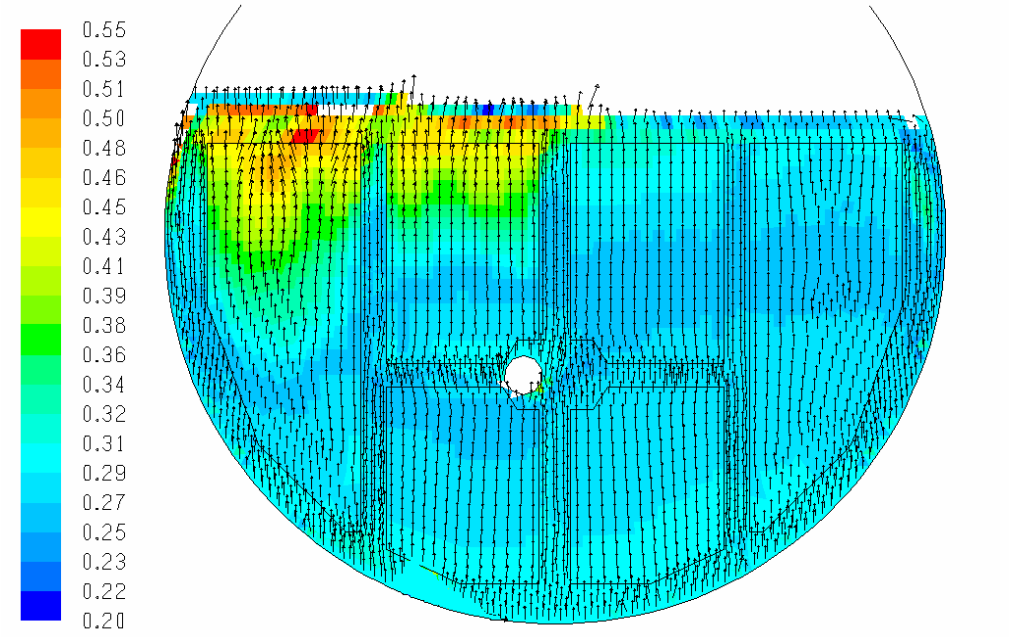

Fig. 5. Distribution of slip velocity [m s^{-1}] in the cross-section of the steam generator.

3.5. Numerical control of water level. Water level is controlled by signals of real time water level measurements in the real technological process. Output signal of the water level probes is proportional to the hydrostatic pressure difference between the higher and the lower taping points of the probe. If the lower taping point is positioned to a height other than the bottom of the tank, which is usually the case, the total mass of liquid water contained by the vessel depends on the steam content under the lower tapping point. The applied mathematical model of multiphase flow ensures mass conservation for the saturated water phase, but the initial mass is unknown due to its dependence on the steam concentration, therefore, a kind of level control must be employed in the numerical simulation as well.

Role of numerical level control is the fastest possible adjustment of the instantaneous water level to a given target level, for that reason, time constant of level control in the numerical system has been chosen to 1 sec, which is much shorter than that in the reality. By the application of an evenly distributed mass source of saturated water the numerical level control has managed to stabilize the instantaneous water level within an error bound of 1 mm after 10 seconds of simulation time.

4. Simulation results. Simulation of the shell side flow in a VVER type steam generator has been carried out for the power load of the original design (224 MW) and for an increased power operation (251 MW) assuming a randomly distributed plugging of heat exchanger tubes. From the simulation results the following conclusions could be drawn:

1. Maximum volume fraction of water vapor in the liquid mixture is about 55%. A well defined surface is formed, above of which, the volume fraction of vapor approaches 100% (see Fig. 8).

2. Highest point of the water surface is located in the vicinity of the hot leg (see Fig. 7), the lowest point (40 cm-s below the highest level) is close those end wall that is at maximum distant from the hot leg. Water surface at the lowest level point approaches (or reaches) the heat exchanger tube bank. Surface shape obtained from the simulation model is in good correlation with earlier experimental observations [3].

3. As can be speculated, the shell side flow is directed upwards on the hot side and downwards on the cold side of the vessel, forming the main circulation pattern in the cross-section of the vessel, visualized in Fig. 6. Moreover an extensive local circulation is present on the cold side as a consequence of large difference between arch lengths and heating intensities of the heat exchanger tubes of inner and outer positions. Similar, but narrower, circulation can be observed on the hot side due to the low hydraulic resistance of the clearance between the vessel wall and the tube bank.

4. Strong circulations take place at both end walls of the vessel (see Fig. 6) caused by the relatively large gap between the wall and the tube bank.

5. The way of feed water injection has a substantial effect on the shell side flow. Fluid characterized by steam content strongly reduced by the feed water injection has a tendency for fast drop down motion. This cold plume can reach the bottom of the vessel even in the case of upper feed water injection. Higher steam content and more intensive circulation has been predicted by the simulation model for high level feed water injection.

6. Results obtained from simulations with two different approximations for the turbulent transport, i.e. constant turbulent viscosity ($\mu_t = 100\mu$) and realizable k–ε model, could be compared for the detailed geometrical model. Only minor differences could be observed in the results, underlining the dominance of multiphase flow effects.

7. Model results from coarse and fine spatial resolutions were very similar too. Surface pattern obtained from the highly resolved model showed better correlation with the measured data.

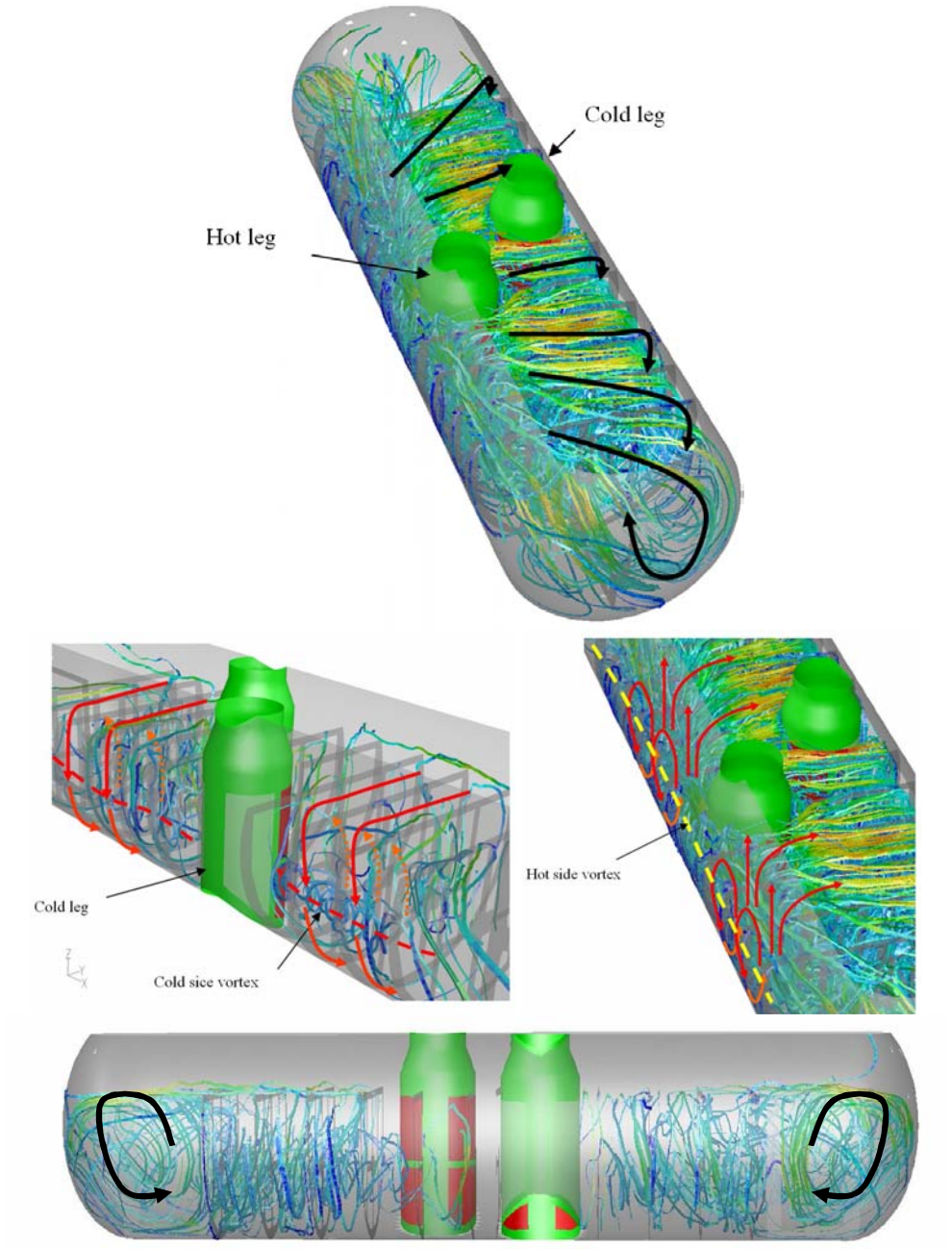

Fig. 6: Stream lines (colored by velocity magnitude) and the main flow features highlighted by heavy arrows.

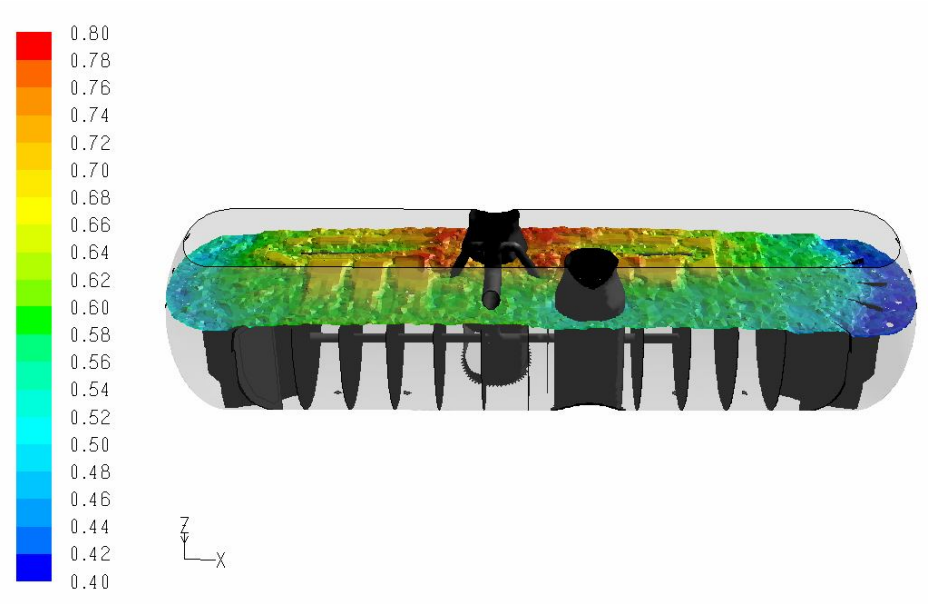

Fig. 7: Water surface elevation [m] defined by the 70% iso-surface of the volume fraction of water vapor.

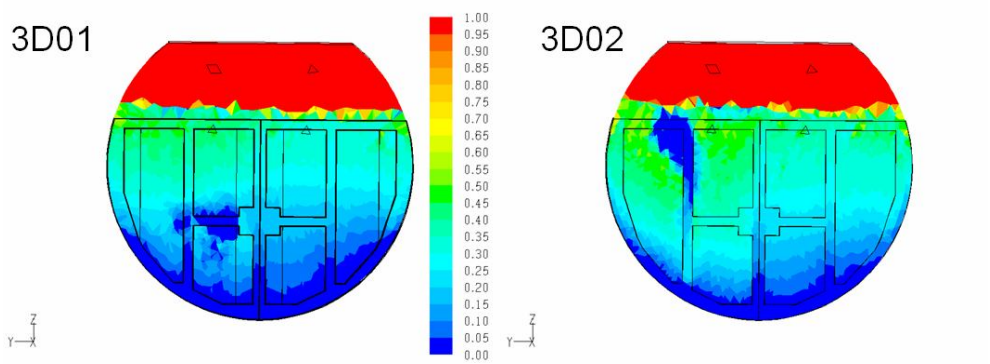

Fig. 8: Volume fraction of gas phase (water vapor) in the cross section 1.5 m away from the symmetry plane with lower (lower) and upper (right) feed water supply.

Резюме

С помощью двумерного и трехмерного геометрических подходов был смоделирован поток теплоносителей в парогенераторах энергоблока ВВЭР-440. Проанализированы следующие рабочие состояния: номинальная и повышенная нагрузки при первоначальной подаче водного питания (внутри трубного пучка) и использование текущего водного питания (над трубным пучком). Математическая модель включает в себя следующие физические явления: тепловое расширение водной фазы, местная конденсация в месте впуска водяного питания, переменная скорость скольжения пузырьковой фазы в зависимости от локальной объемной доли пара, пространственное изменение

уровня воды над трубным пучком и оседание дисперсных продуктов коррозии под трубным пучком. Разработаны микро модели для расчета анизотропного сопротивления пучка труб и опор трубопроводов, локального теплового потока по поверхности труб и пространственные изменения интенсивности подачи воды. Уровень воды и осаждение дисперсной фазы в соответствии с данными измерений опубликованы в научной литературе [3] и [4].

Ключевые слова: моделирование, двухфазный поток, парогенератор, ВВЭР-440.

Резюме

З допомогою двомірного и трьохмірного геометричних підходів змодельовано потік теплоносіїв в парогенераторах енергоблока ВВЕР-440. Проаналізовано наступні рабочі стани: номінальне і підвищене навантаження при первинній подачі водяного живлення (всередині трубного пучка) і використання поточного водяного живлення (над трубним пучком). Математична модель містить в собі наступні фізичні явища: теплове розширення водяної фази, місцеву конденсацію в місці впуску водяного живлення, змінна швидкість ковзання бульбашкової фази в залежності від локальної об'ємної частки пари, просторова зміна рівня води над трубним пучком і осідання дисперсних продуктів корозії під трубним пучком. Розроблено мікро моделі для розрахунку анізотропного опору пучка труб і опор трубопроводів, локального теплового потоку по поверхні труб і просторові зміни інтенсивності подачі води. Рівень води і осад дисперсної фази у відповідності з даними вимірювань опубліковані в науковій літературі [3] і [4].

Ключові слова: моделювання, двохфазний потік, парогенератор, ВВЕР-440.

1. *Stosic Z., Stevanovic V.* Advanced three-dimensional two-fluid porose media method for transient two-phase flow thermal-hydraulics in complex geometries // Numer. Heat Transfer. – 2002. – **A 41**. – P. 263 – 289.
2. *Pezo M., Stevanovic V. D., Stevanovic Z.* A two-dimensional model of the kettle reboiler shell side thermal-hydraulics // Int. J. Heat Mass Transfer. – 2006. – **49.** – P. 1214 – 1224.
3. *Dmitrijev A. I., Kozlov Ju. V. et. al.* Opyt ispolzovaniya zhalyuznyh separatorov v sisteme AES // Teploenergetika. – 1989. – **12**. – P. 11 – 14.
4. *Beljakov V. A., Szmirnov Sz. V.* Analiz i ocenka dannyh VTK teploobmennyh trub parogeneratorov Kolskoj AES. – Proceedings of the 7-th International Seminar on Horizontal Steam Generators, 3-5 October, 2006, Podolsk, Section 1: Operational experience, inspection and life management.
5. *Ősz J., Tajti T., Kaszás Cs*: A VVER-440 gőzfejlesztők megbízhatósága és hatekonyabb leiszapolasa a PA-ben. Magyar Energetika 2008 / (megjelenes alatt).

Поступила 20.05.2009